

Downregulation of *circ_0119412* expression inhibits malignant progression of breast cancer by targeting the *miR-1205/GALNT6* pathway *in vivo* and *in vitro*

Jianhua Liu, Qiuli Du, Yong Yang*

Department of Thyroid and Breast Surgery, Wuhan No. 1 Hospital (Wuhan Chinese and Western Medicine Hospital), Wuhan, Hubei, China

Submitted: 7 November 2022; **Accepted:** 22 April 2023

Online publication: 16 January 2024

Arch Med Sci 2025; 21 (3): 974–990
DOI: <https://doi.org/10.5114/aoms/163530>
Copyright © 2024 Termedia & Banach

Abstract

Introduction: Aberrant circular RNA (circRNA) expression is associated with development of breast cancer. In this study, we aimed to assess the anti-proliferative effect of *circ_0119412* knockdown on breast cancer cells.

Material and methods: Tumor and adjacent normal tissues were collected from 35 patients with invasive breast cancer (mean age: 56 years; mean tumor size: 2 cm; 46% patients with TNM I and II stages). The levels of *circ_0119412*, microRNA (*miR*)-1205, and N-acetylgalactosaminyltransferase 6 (*GALNT6*) were determined using reverse transcription-quantitative polymerase chain reaction. Cell proliferation and invasion were assessed using cell counting kit-8 and transwell assays, respectively. Cell apoptosis was assessed using flow cytometry. Moreover, the targeting relationships of *miR-1205* with *circ_0119412* and *GALNT6* were determined using dual-luciferase reporter and RNA immunoprecipitation assays. Furthermore, tumor growth was observed in an animal model *in vivo*.

Results: We found that *circ_0119412* expression levels were upregulated in breast cancer tumor specimens and cell lines. Downregulation of *circ_0119412* inhibited the invasion and proliferation, while enhancing the apoptosis of breast cancer cells. Furthermore, *circ_0119412* knockdown suppressed tumor growth *in vivo*. Notably, *miR-1205* was identified as a downstream target of *circ_0119412*. Downregulation of *circ_0119412* suppressed the aggressive behavior of breast cancer cells by targeting *miR-1205*. Moreover, *GALNT6* was the downstream target of *miR-1205*. Inhibition of *miR-1205* aggravated the malignant behavior of breast cancer cells by increasing *GALNT6* expression.

Conclusions: Our findings suggest that the downregulation of *circ_0119412* inhibits breast cancer progression, at least in part, by targeting the *miR-1205/GALNT6* pathway.

Key words: *circ_0119412*, breast cancer, *miR-1205*, *GALNT6*.

*Corresponding author:

Yong Yang
Department of Thyroid and Breast Surgery
Wuhan No. 1 Hospital
Wuhan Chinese and Western Medicine Hospital
No. 215, Zhongshan Avenue
Qiaokou District
Wuhan 430022
Hubei, China
Phone/fax: +86 13808608768
E-mail: yongyang63@163.com

Introduction

Breast cancer is the most frequently diagnosed cancer in women, accounting for 11.7% of all newly diagnosed cancer cases in 2020 [1]. Timely detection and treatment are necessary to improve the treatment response and prognosis of patients with breast cancer. However, breast cancer has a higher mortality rate owing to late diagnosis, chemotherapy resistance, and metastasis [2, 3]. Breast cancer is a highly heterogeneous

disease with unique and complex histopathological patterns and clinical behaviors [4, 5]. Moreover, breast cancer pathogenesis is complex and poorly understood. Several studies have reported specific tumor markers for the evaluation of cancer progression [6]. Analysis of biomarkers is essential for the early diagnosis and adequate treatment of breast cancer.

Circular RNAs (circRNAs) have gained increasing attention owing to their involvement in cancer progression. CircRNAs are special non-coding RNAs with closed-loop structures that lack 5'- and 3'-ends [7]; however, their specific roles in diseases remain ambiguous. Deregulation of circRNAs is associated with the development and progression of various diseases, including cancer [8, 9]. Previous studies have reported several circRNAs with potential diagnostic value, whose aberrant expression is associated with advanced tumor stages and poor prognosis and therapeutic response in patients with breast cancer [10–12]. Moreover, several circRNAs have been reported to modulate cancer cell phenotypes and functions, such as proliferation, apoptosis, energy metabolism, and metastasis [13, 14]. Several circRNAs have been identified owing to the advancement in RNA sequencing technology; however, the functions of most circRNAs remain unknown. *Hsa_circ_0119412* and *circRNA_102958* levels were initially reported to be upregulated in gastric cancer using circRNA microarray data [15]. We also observed increased *circRNA_0119412* expression levels in breast tumor tissues in our study, suggesting that *circ_0119412* may be involved in breast cancer development. However, the specific functions and underlying molecular mechanisms of *circ_0119412* in breast cancer remain unclear.

CircRNAs containing microRNA (miRNA) response elements may function as sponges of their target miRNAs to modulate their expression [16]. Advancements in bioinformatics have facilitated the prediction of miRNAs bound to circRNAs [17]. In this study, we determined the functional mechanisms of *circ_0119412* by assessing its target miRNA, *miR-1205*. *miR-1205* expression is downregulated in various cancers [18, 19]. miRNAs modulate the expression of genes by targeting their 3'-untranslated regions (UTRs) [20]. Bioinformatics analysis has revealed that *miR-1205* contains complementary sequences of polypeptide N-acetylgalactosaminyltransferase 6 (*GALNT6*) 3'-UTR, suggesting that *miR-1205* may mediate *GALNT6* silencing. *GALNT6* mediates the initial steps of mucin-type O-glycosylation [21]. *GALNT6* also promotes carcinogenesis in various cancers [21–23]. However, the mechanism by which the interaction of *GALNT6* with *miR-1205* affects the development of breast cancer remains unknown.

In this study, we determined the expression levels and functions of *circ_0119412* in breast cancer cells and tumor specimens of an animal model. We also assessed the associations of *miR-1205* with *circ_0119412* and *GALNT6* and their influence on breast cancer development. Our study aimed to determine the anti-proliferative effect of *circ_0119412* knockdown on breast cancer cells. To the best of our knowledge, this study is the first to examine the roles of *circ_0119412* in breast cancer.

Material and methods

Tissue specimens

Tumor ($n = 35$) and normal (non-cancerous; $n = 35$) specimens were collected during surgery from the female patients with breast cancer enrolled in our hospital. All patients provided written consent prior to their participation in this study. Inclusion criteria were as follows: 1) patients diagnosed with breast cancer and 2) patients or their family members providing written consent. Exclusion criteria were as follows: 1) patients without a history of breast cancer, 2) patients who underwent therapy before surgery, and 3) patients with other diseases. This study was designed and conducted with approval from our hospital. Characteristics of all patients with breast cancer included in this study are listed in Table I.

Cell lines and cell culture

Common breast cancer (MDA-MB-231, MCF-7, and MDA-MB-468) and normal breast epithelial (MCF-10A) cell lines were purchased from Procell (Wuhan, China). MCF-7 and MCF-10A cells were cultured in Dulbecco's modified Eagle's medium (Gibco, USA) containing 10% fetal bovine serum (FBS). MDA-MB-468 and MDA-MB-231 cells were

Table I. Characteristics of patients with breast cancer

Characteristics	Cases
Age:	
≥ 56	18
< 56	17
Tumor size:	
≥ 2 cm	20
< 2 cm	15
TNM stage:	
I–II	16
III–IV	19
Tumor type:	
Invasive ductal carcinoma	22
Invasive lobular carcinoma	13

Table II. Real-time PCR primer sequences

Gene name	Sequence
hsa_circ_0119412	Forward 5'-GACGCCCTACCTGGTCAAG-3' Reverse 5'-GAAATTCGCGTATCCATTC-3'
miR-1205	Forward 5'-GCCGAGCGTTTGGGACGTCT-3' Reverse 5'-CAGTGCCTGCTGGAGT-3'
GALNT6	Forward 5'-AGAGAAATCCTTCGGTGACATT-3' Reverse 5'-AGACAAAGSGCCACAACCTGATG-3'
GAPDH	Forward 5'-GAACATCATCCCTGCCTTACT-3' Reverse 5'-CCTGCTTACCACCTTCTTG-3'
U6	Forward 5'-GCTTCGGCAGCACATACTAAAAT-3' Reverse 5'-CGTTCACGAATTTGCGTGCAT-3'
CDC45	Forward 5'-AGAAAGTCAGGCGTTCTACAG-3' Reverse 5'-GGGAGATTCAGGGAGAGTCAT-3'
HIST1H2BK	Forward 5'-CACCAGCGCTAAGTAACTTGCCA-3' Reverse 5'-AGAGGCCAGCTTAGCTTGTGGAA-3'
GATA3	Forward 5'-GAGATGGCAGGGACACTACCT-3' Reverse 5'-GTGGTGGTCTGACAGTTGCG-3'

GALNT6 – polypeptide *N*-acetylgalactosaminyltransferase 6, *CDC45* – cell division cycle associated 5, *HIST1H2BK* – H2B clustered histone 12, *GATA3* – GATA binding protein 3.

cultured in Leibovitz's L-15 medium (Gibco) containing 10% FBS. Cultures were incubated at 37°C and 5% CO₂.

Reverse transcription-quantitative polymerase chain reaction (RT-qPCR)

Total RNA was isolated from cells using the Trizol reagent and analyzed using NanoDrop2000 (Thermo Fisher Scientific, USA). Then, total RNA was reverse-transcribed into cDNA using the iScript cDNA Synthesis Kit (Bio-Rad, USA) and miRNA Reverse Transcription Kit (Qiagen, Germany), according to the manufacturers' protocols. cDNA was then amplified via qPCR using the QuantiTect SYBR Green PCR Kit (Qiagen) and LightCycler 96 thermocycler (Roche, Switzerland). Relative expression levels of genes were normalized against uracil 6 (*U6*) or glyceraldehyde 3-phosphate dehydrogenase (*GAPDH*) levels using the 2^{-ΔΔCT} method. All primer sequences used in this study are listed in Table II.

Subcellular localization

The Cytoplasmic and Nuclear RNA Purification Kit (Norgen Biotek, Canada) was used to isolate RNAs from the cytoplasm and nucleus, and enrichment of *circ_0119412* in each fraction was assessed using RT-qPCR. As *GAPDH* is mainly located in the cytoplasm and *U6* is mainly located in the nucleus, *GAPDH* was used as the cytoplasmic control, and *U6* was used as the nuclear control.

RNase R treatment

RNA samples were treated with RNase R (2 U/μg; BioVision, USA) and subjected to RT-qPCR to

assess the changes in the expression levels of *circ_0119412* and the linear gene period circadian regulator 2 (*PER2*).

Cell transfection

Oligonucleotides for *circ_0119412* silencing (si-*circ*) and its matched negative control (si-NC) were obtained from GenePharma (China). miR-1205 mimic, miR-1205 inhibitor, mimic-NC, and inhibitor-NC were purchased directly from RiboBio (China). Oligonucleotides against *GALNT6* (si-*GALNT6*) and its matched negative control (si-NC) were also purchased from GenePharma. Then, the oligonucleotides were transfected individually or in specific combinations into the experimental cells using the Lipofectamine 3000 reagent (Invitrogen, China). After 24 h, cells were collected and the transfection efficiency was determined via RT-qPCR and western blotting.

Cell counting kit (CCK)-8 assay

Transfected cells were seeded in a 96-well plate at a density of 5,000 cells/well. After culturing at 37°C for 0, 24, 48, and 72 h, the cells in each well were mixed with the CCK-8 reagent (Invitrogen) and maintained for another 4 h. Cell viability was determined based on the absorbance at 450 nm using a microplate reader (Bio-Rad).

Transwell assay

Transwell chambers (Corning, USA) pretreated with Matrigel (Corning) were used for cell invasion analysis. Transfected cells were cultured for 24 h, collected in a serum-depleted medium, and transferred to the top transwell chambers. A fresh

culture medium containing 20% FBS was added to the bottom chamber. Cells were allowed to invade the membrane for 24 h. Cells that invaded the lower surface of the membranes were immobilized with methanol and stained with crystal violet. Cell morphology was observed under a light microscope (Leica, Germany).

Flow cytometry assay

Transfected cells were cultured for 48 h and collected after trypsin digestion. An Annexin V-FITC/PI Apoptosis Detection Kit (Vazyme, China) was used to identify the apoptotic cells. Briefly, cells were resuspended in Annexin V-FITC binding buffer and stained with annexin V-FITC and propidium iodide. Then, a flow cytometer (Beckman Coulter, USA) was used to estimate the cell apoptosis rate.

Animal study

Six-week-old female nude mice were purchased from Beijing Charles River Laboratories (China). Geneseeed (China) assembled the lentiviruses of short hairpin RNAs targeting *circ_0119412* (sh-*circ*) or *GALNT6* (sh-*GALNT6*) and *miR-1205* overexpression (Lv-*miR-1205*) and their negative controls (sh-NC and Lv-NC, respectively). MCF-7 cells were transfected with either sh-*circ* or sh-NC lentiviral vectors, and 2×10^6 cells were subcutaneously injected into each nude mouse ($n = 5$ per group) to induce tumor formation. Tumor volume (length \times width² \times 0.5) was recorded weekly for 5 weeks, after which the mice were sacrificed to excise the tumors for analyses. All animal experimental procedures used in this study were approved by our hospital.

Dual-luciferase reporter assay

Mutant (MUT) and wild-type (WT) *circ_0119412* reporter plasmids were generated using the pmir-GLO plasmid (Promega, USA). Moreover, WT and MUT *GALNT6* reporter plasmids were constructed in a similar manner. As *miR-1205* and *GALNT6* share two binding sites, various *GALNT6* reporter plasmids, namely WT, Co-MUT (mutations at two sites), MUT1 (mutation at one site), and MUT2 (mutation at the other site) plasmids, were constructed and transfected with the *miR-1205* or NC mimic into MDA-MB-231 and MCF-7 cells. After 48 h, luciferase activity was determined using the Dual-Luciferase Reporter Assay System (Promega).

RNA immunoprecipitation (RIP) assay

The Imprint RNA Immunoprecipitation Kit and experimental (anti-IgG and anti-Ago2) antibodies were acquired from Sigma-Aldrich (USA). MDA-MB-231 and MCF-7 cells were treated with the

RIP lysis buffer, and cell lysates were incubated with Protein A Magnetic Beads pre-coated with anti-IgG or anti-Ago2. Then, RNA complexes were washed and purified. Finally, RT-qPCR was performed to quantify the expression levels of *miR-1205* and *circ_0119412*.

Western blotting

Total protein was extracted from the cells using the radioimmunoprecipitation assay lysis reagent (Beyotime, Shanghai, China). Proteins were quantified using a BCA kit (Beyotime). After separation using 12% sodium dodecyl sulfate-polyacrylamide gel electrophoresis, the protein bands were transferred to polyvinylidene fluoride membranes (Beyotime), blocked with 5% skim milk for 1 h at room temperature, and incubated with primary antibodies against GAPDH (1 : 2500 dilution; ab181602; Abcam, USA) and *GALNT6* (1 : 1000 dilution; ab151329; Abcam) at 4°C overnight, followed by incubation with secondary antibodies (1 : 10000 dilution; ab205718; Abcam) for 2 h at room temperature. Finally, an ECL kit (Beyotime) was used to visualize the protein bands.

Statistical analysis

Each assay was performed in triplicate. GraphPad Prism v7.0 (GraphPad Software, USA) was used to process the data and construct the graphs. Pearson's rank correlation was used to ascertain the correlation between groups. Student's *t*-test was used to compare two groups. Analysis of variance with post-hoc Tukey's correction was used for multigroup comparisons. Data are presented as the mean \pm standard deviation. Statistical significance was set at $p < 0.05$.

Results

Circ_0119412 expression levels are increased in breast cancer cell lines and tumor specimens

First, we determined *circ_0119412* expression in breast cancer. As depicted in Figures 1 A and B, *circ_0119412* levels were markedly higher in the breast cancer specimens and (MDA-MB-231, MCF-7, and MDA-MB-468) cell lines than in the normal specimens and non-cancerous (MCF-10A) cell lines (tumor:normal = 2.91, MDA-MB-231:MCF-10A = 3.39, MCF-7:MCF-10A = 3.95, and MDA-MB-468:MCF-10A = 1.57). As MDA-MB-231 and MCF-7 cells exhibited the highest *circ_0119412* expression, they were selected for subsequent experiments. CircRNA subcellular localization analysis revealed that relative to the nucleus, *circ_0119412* was mainly and abundantly distributed in the cytoplasm (approximately 60%)

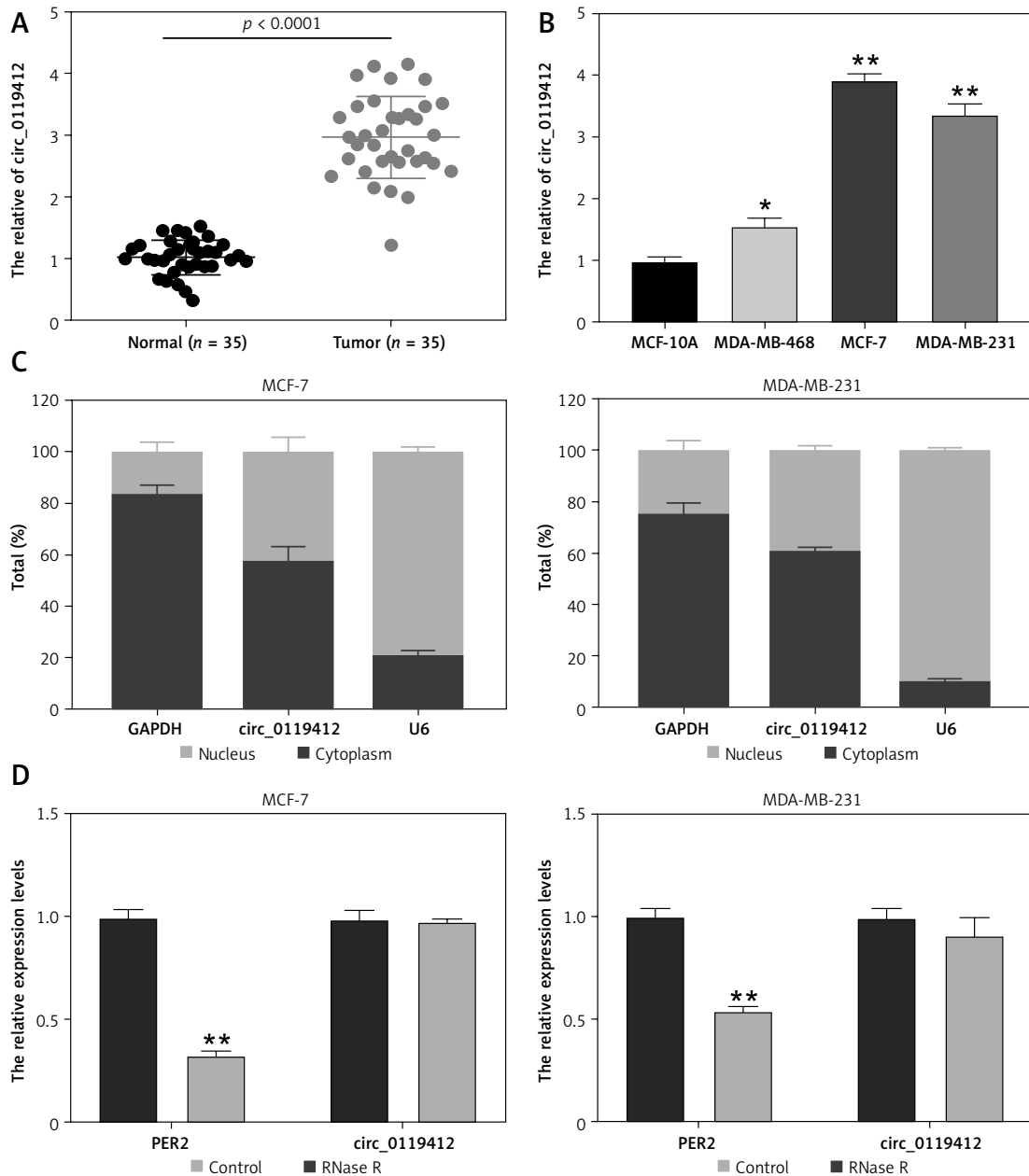


Figure 1. Increased circ_0119412 expression was detected in the breast cancer cell lines and tumor specimens. **A** – Circ_0119412 expression in tumoral and normal samples was checked via RT-qPCR. **B** – The circ_0119412 expression levels in MDA-MB-231, MCF-10A, MCF-7, and MDA-MB-468 cells were quantified by means of RT-qPCR, * $P < 0.05$, ** $p < 0.001$ vs. MCF-10A. **C** – The circ_0119412 expression levels within the cytoplasm and nuclei of the cells were determined via RT-qPCR. **D** – The presence of circ_0119412 was confirmed by treating the RNA with RNase R, ** $p < 0.001$ vs. Control

of breast cancer cells (Figure 1 C). RNase R was used to digest the total RNA extracted from cells to confirm the presence of circ_0119412. RNase R barely affected the expression of circ_0119412 but substantially decreased the expression of its linear parental gene, PER2 (Figure 1 D). These results indicate that circ_0119412 dysregulation may be associated with breast cancer development.

Circ_0119412 deficiency inhibits aggressive breast cancer development *in vitro* and *in vivo*

To determine the functions of circ_0119412, we downregulated its expression in MCF-7 and MDA-MB-231 cells. circ_0119412 expression levels were markedly lower in cell lines transfected with si-circ than in those transfected with si-NC ($p < 0.001$; Figure 2 A). CCK-8 assay revealed lower proliferation rates in MCF-7 and MDA-MB-231 cells transfected with si-circ than in those trans-

fectured with si-NC ($p < 0.001$; Figure 2 B). Moreover, transwell assay revealed considerably lower invasion rates in cancer cells transfected with si-circ than in those transfected with si-NC ($p < 0.001$, Figure 2 C). However, *circ_0119412*

silencing reversed these effects ($p < 0.001$; Figure 2 D). Furthermore, animal models were established by injecting sh-circ- or sh-NC-transfected MCF-7 cells into nude mice. Compared with the sh-NC-administered group, tumor sizes and

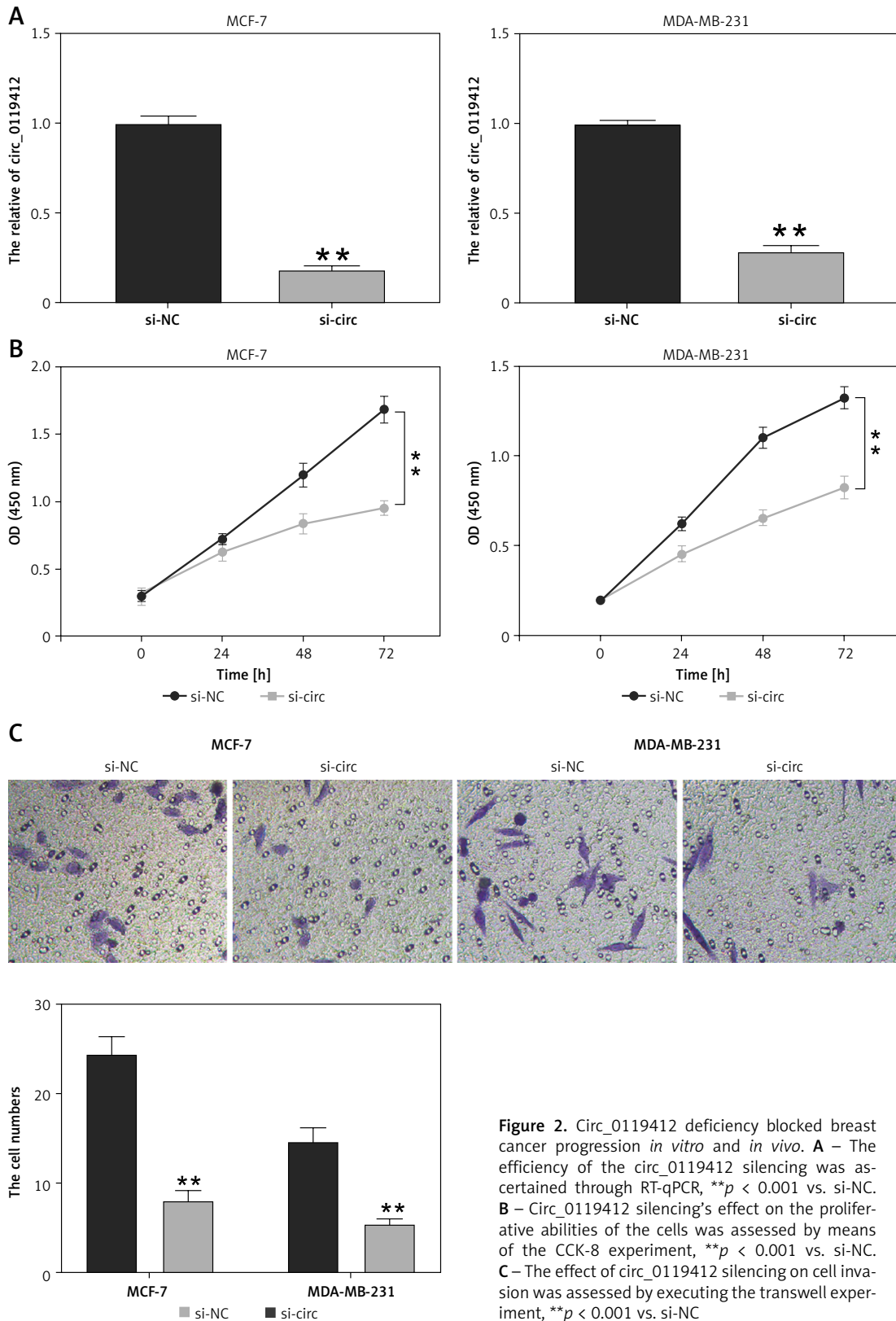


Figure 2. Circ_0119412 deficiency blocked breast cancer progression *in vitro* and *in vivo*. **A** – The efficiency of the circ_0119412 silencing was ascertained through RT-qPCR, $**p < 0.001$ vs. si-NC. **B** – Circ_0119412 silencing's effect on the proliferative abilities of the cells was assessed by means of the CCK-8 experiment, $**p < 0.001$ vs. si-NC. **C** – The effect of circ_0119412 silencing on cell invasion was assessed by executing the transwell experiment, $**p < 0.001$ vs. si-NC

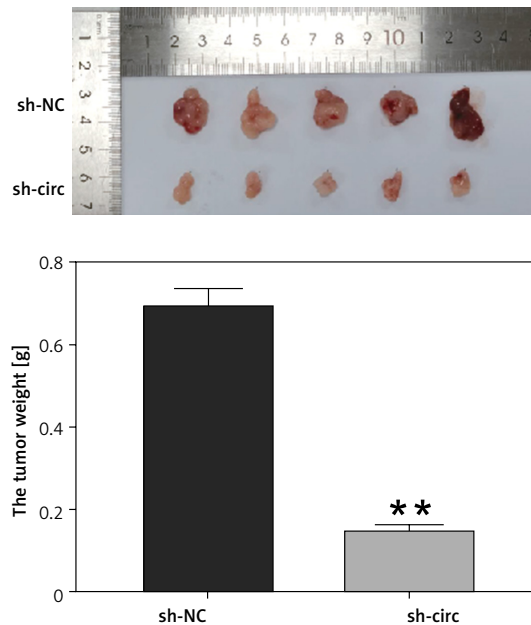
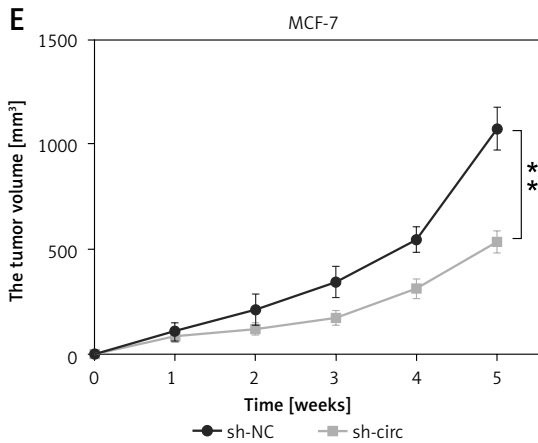
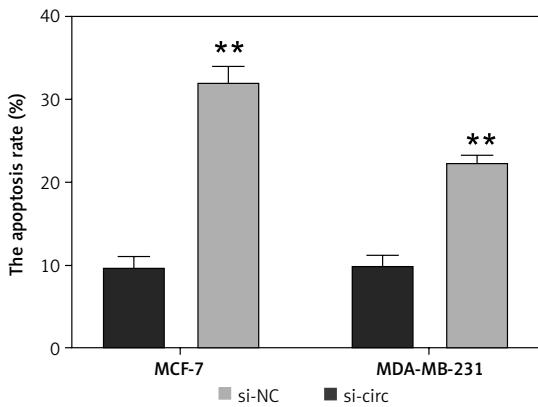
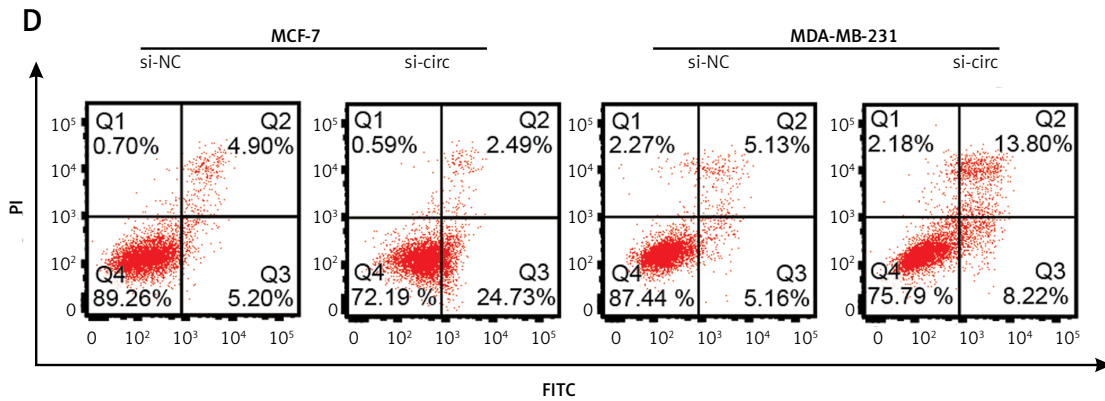


Figure 2. Cont. **D** – The effect of *circ_0119412* silencing on apoptosis was determined via flow cytometry, ** $p < 0.001$ vs. si-NC. **E** – The animal study was conducted to assess how *circ_0119412* knock-down affected the growth of solid tumors *in vivo*, ** $p < 0.001$ vs. sh-NC

weights were lower in the sh-circ-administered group ($p < 0.001$; Figure 2 E). Collectively, these results suggest that *circ_0119412* deficiency inhibits breast cancer progression.

miR-1205 is a downstream target of *circ_0119412*

CircInteractome prediction revealed that *circ_0119412* possessed an *miR-1205*-binding

site (Figure 3 A). Dual-luciferase reporter assay demonstrated that restoring *miR-1205* expression considerably decreased the luciferase activity in MCF-7 and MDA-MB-231 cells containing the *circ_0119412* WT reporter plasmid compared to that in cells containing the MUT plasmid ($p < 0.001$; Figure 3 B). RIP assay revealed that *miR-1205* and *circ_0119412* were more abundant in the anti-Ago2-enriched RIP group than in the anti-IgG-enriched RIP group ($p < 0.001$; Figure 3 C).

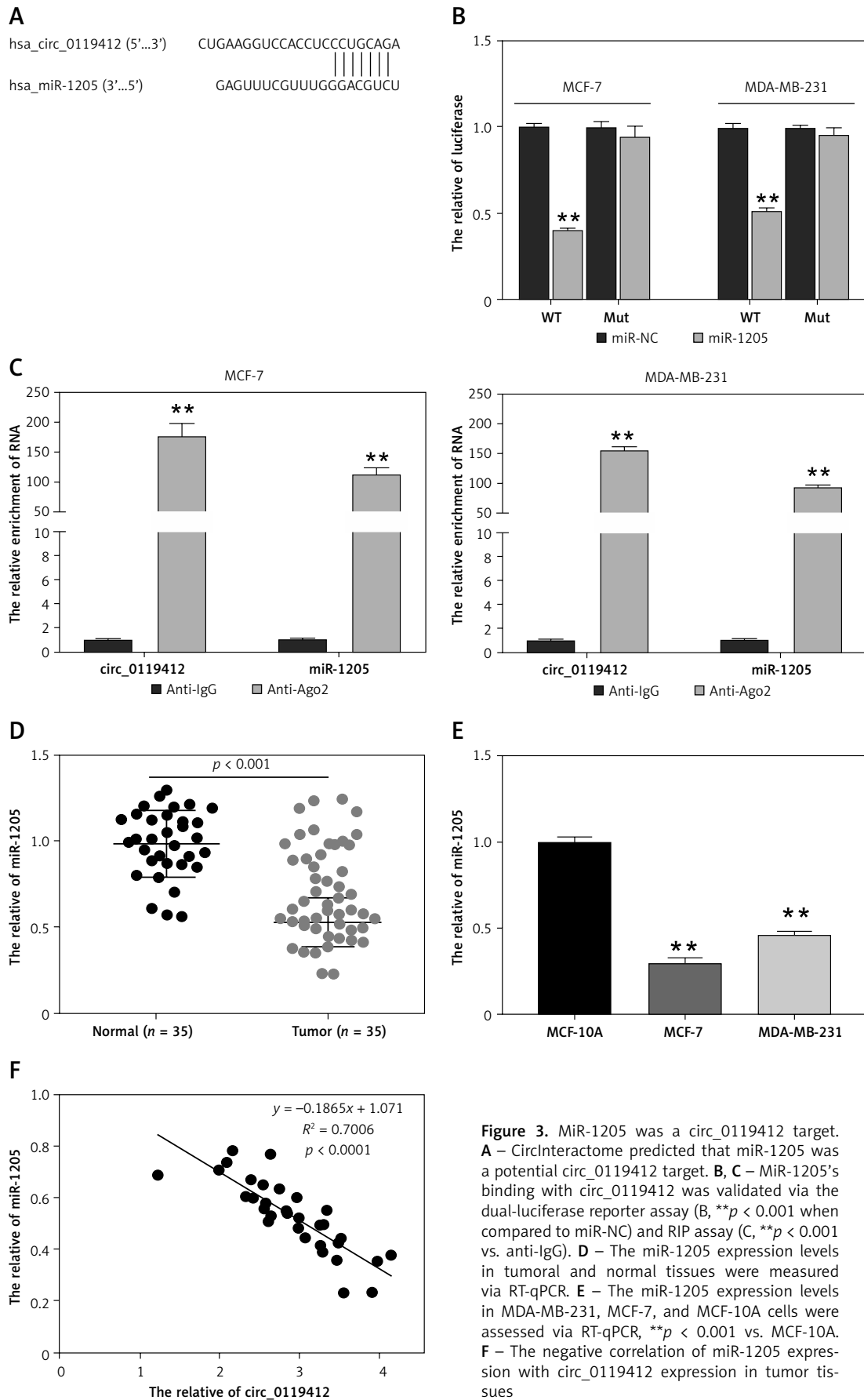


Figure 3. MiR-1205 was a *circ_0119412* target. **A** – CircInteractome predicted that miR-1205 was a potential *circ_0119412* target. **B, C** – MiR-1205's binding with *circ_0119412* was validated via the dual-luciferase reporter assay (B, $**p < 0.001$ when compared to miR-NC) and RIP assay (C, $**p < 0.001$ vs. anti-IgG). **D** – The miR-1205 expression levels in tumoral and normal tissues were measured via RT-qPCR. **E** – The miR-1205 expression levels in MDA-MB-231, MCF-7, and MCF-10A cells were assessed via RT-qPCR, $**p < 0.001$ vs. MCF-10A. **F** – The negative correlation of miR-1205 expression with *circ_0119412* expression in tumor tissues

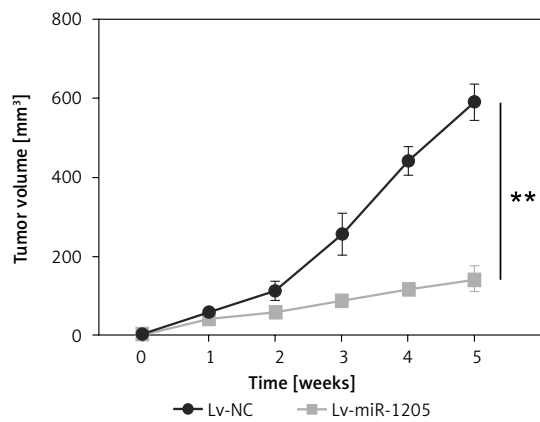
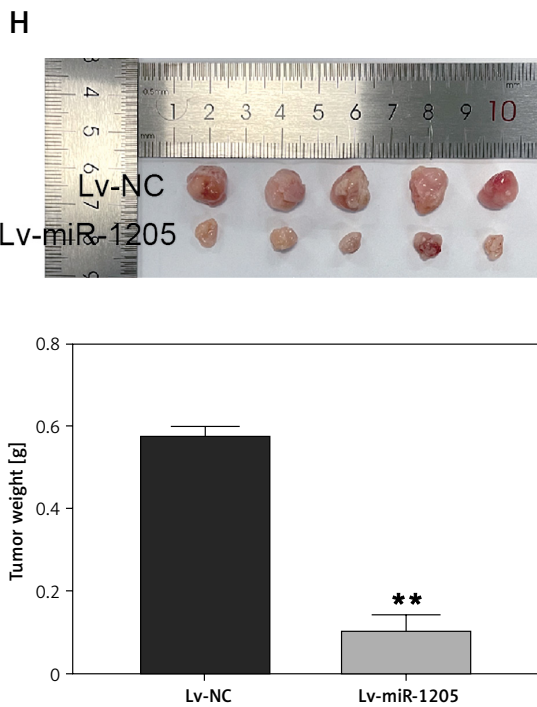
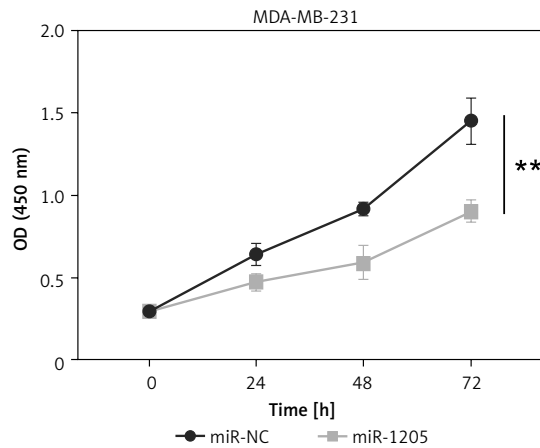
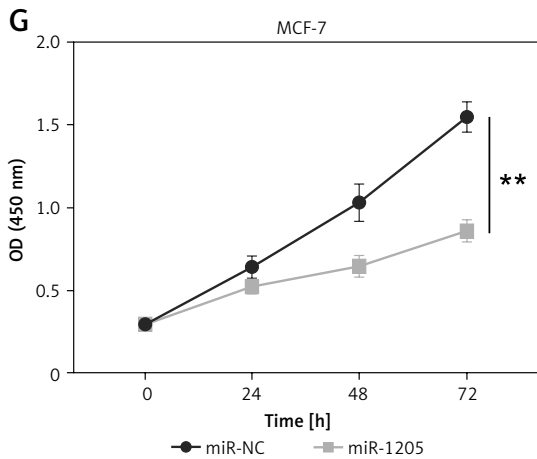
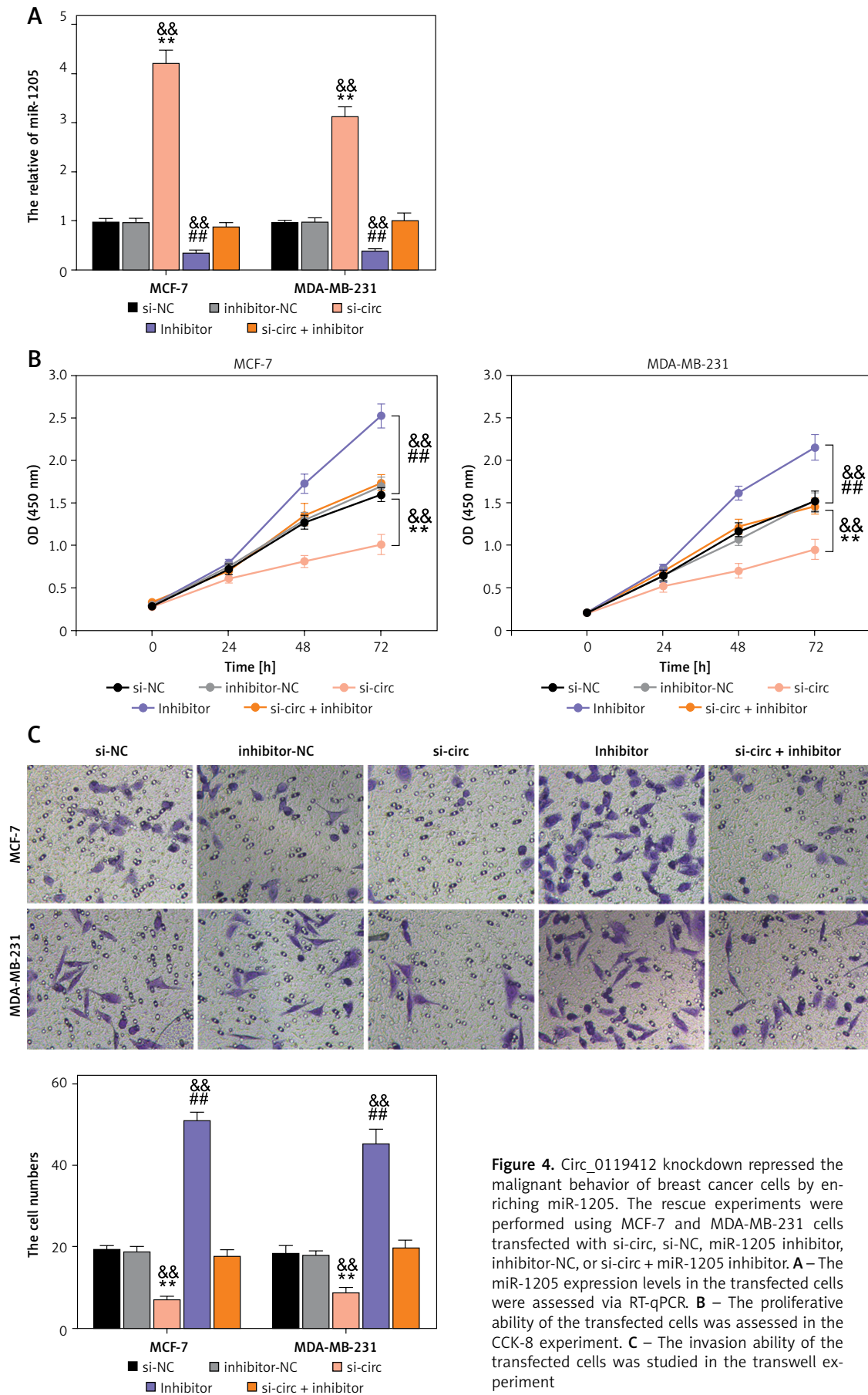


Figure 3. Cont. **G** – miR-1205 overexpression’s effect on the proliferative abilities of the cells was assessed by means of the CCK-8 experiment, ** $p < 0.001$ vs. miR-NC. **H** – The animal study was conducted to assess how miR-1205 overexpression affected the growth of solid tumors *in vivo*, ** $p < 0.001$ vs. Lv-NC

Further expression analysis revealed considerably lower *miR-1205* expression levels in breast cancer tumor specimens and cell lines (MDA-MB-231 and MCF-7) than in normal specimens and cell lines (MCF-10A) (tumor : normal = 0.54, MDA-MB-231:MCF-10A = 0.30, and MCF-7 : MCF-10A = 0.46; Figures 3 D and E). Furthermore, *miR-1205* expression was inversely correlated with *circ_0119412* expression in breast cancer tissues (Figure 3 F). CCK8 assay confirmed that *miR-1205* overexpression significantly inhibited cancer cell proliferation *in vitro* ($p < 0.001$; Figure 3 G). The *in vivo* experiment revealed that *miR-1205* overexpression reduced the tumor volumes and weights in mice ($p < 0.001$; Figure 3 H). Overall, these results suggest that *circ_0119412* targets *miR-1205*.

Circ_0119412 knockdown inhibits breast cancer development by increasing *miR-1205* expression

To assess the impact of the interplay between *miR-1205* and *circ_0119412* on breast cancer progression, rescue experiments were performed using MCF-7 and MDA-MB-231 cells. si-circ, miR-1205 inhibitor, or their combination (si-circ + miR-1205 inhibitor) was transfected into the cells. *miR-1205* expression was remarkably elevated by si-circ but decreased by the miR-1205 inhibitor ($p < 0.001$; Figure 4 A). Moreover, transfection with si-circ + the miR-1205 inhibitor reduced the expression of *miR-1205* compared with transfection with si-circ alone. CCK-8 and transwell assays revealed that the proliferative and invasive capacities of MCF-7 and MDA-MB-231 cells were decreased by si-circ and promoted by the miR-



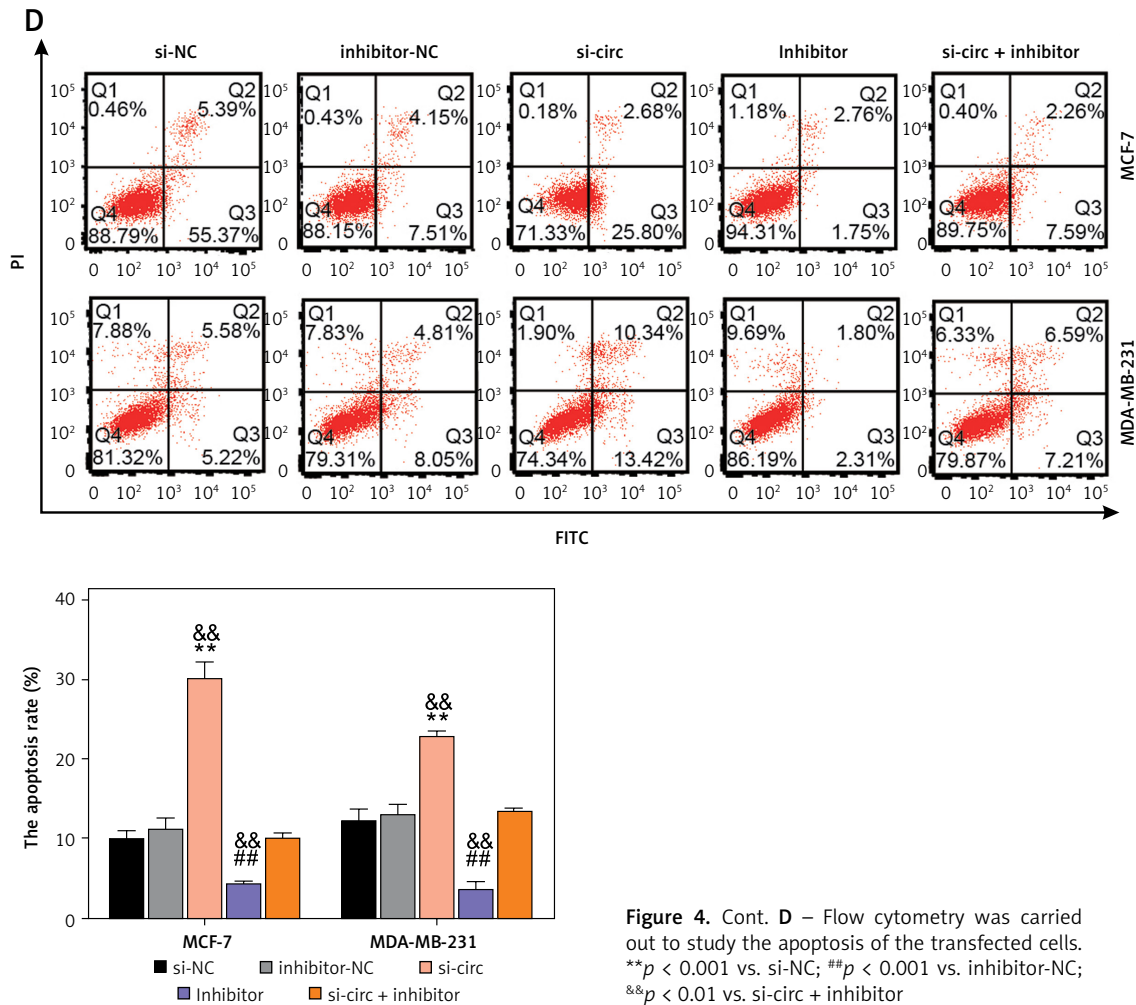


Figure 4. Cont. D – Flow cytometry was carried out to study the apoptosis of the transfected cells. ** $p < 0.001$ vs. si-NC; ## $p < 0.001$ vs. inhibitor-NC; && $p < 0.01$ vs. si-circ + inhibitor

1205 inhibitor ($p < 0.001$, Figures 4 B and C). Furthermore, suppression of cell invasion and proliferation by *circ_0119412* knockdown was partially offset by *miR-1205* inhibition. In addition, cell apoptosis was promoted by si-circ transfection but suppressed by *miR-1205* inhibitor transfection ($p < 0.001$; Figure 4 D). Increased apoptosis induced by *circ_0119412* knockdown was partially repressed by the inhibition of *miR-1205*. Overall, these results indicate that *circ_0119412* knockdown abrogates the malignant behaviors of breast cancer cells via *miR-1205* enrichment.

GALNT6 is a target gene of miR-1205

miRDB and TargetScan were used to identify the downstream targets of *miR-1205*. Gene Expression Profiling Interactive Analysis was used to screen the upregulated genes, with $\log_{2}FC > 2$ and $adj.p < 0.01$. Four genes (cell division cycle-associated 5 [*CDCA5*], *GALNT6*, H2B clustered histone 12 [*H2BC12*, also known as *HIST1H2BK*], and GATA-binding protein 3 [*GATA3*]) were found to be overlapping using Venny 2.1.0 (Figure 5 A). Next, we determined their expression levels in

clinical tumor specimens. *GALNT6* exhibited the highest expression levels in breast cancer tumor specimens (*CDCA5*: upregulated by 1.13-fold, *GALNT6*: upregulated by 6.10-fold, *HIST1H2BK*: upregulated by 1.15-fold, and *GATA3*: upregulated by 1.23-fold; Figure 5 B); hence, it was chosen for further analyses. TargetScan revealed two *miR-1205*-binding sites on the *GALNT6* 3'-UTR sequence fragment (Figure 5 C). *GALNT6* WT and MUT reporter plasmids were synthesized and used in a dual-luciferase reporter assay. Combined transfection with the *GALNT6* WT reporter plasmid and *miR-1205* mimic remarkably diminished the luciferase activity, whereas transfection with the MUT1 + *miR-1205* mimic and MUT2 + *miR-1205* mimic only partially diminished the luciferase activity in cells ($p < 0.001$; Figure 5 D). Moreover, co-transfection with the Co-MUT + *miR-1205* mimic barely reduced the luciferase activity in cells ($p > 0.05$, Figure 5 D). *GALNT6* mRNA expression levels were markedly higher in MCF-7 and MDA-MB-231 cells than in MCF-10A cells ($p < 0.001$; Figure 5 E). Notably, *miR-1205* expression was negatively associated with *GALNT6* mRNA expression in tumor tissues (Figure 5 F). CCK8 assay

revealed that *GALNT6* knockdown significantly inhibited cell proliferation *in vitro* ($p < 0.001$; Figure 5 G). Moreover, *GALNT6* knockdown decreased the tumor volumes and weights *in vivo* (Figure 5 H). These results indicate that *GALNT6* is a target gene of *miR-1205*.

***miR-1205* inhibition aggravates the malignant behaviors of breast cancer cells by increasing *GALNT6* expression**

Next, to assess the impact of the interaction between *miR-1205* and *GALNT6* on breast cancer

progression, rescue experiments were performed using MCF-7 and MDA-MB-231 cells. si-GALNT6, miR-1205 inhibitor, or their combination (si-GALNT6 + miR-1205 inhibitor) was introduced into the cells. *GALNT6* protein expression levels in MCF-7 and MDA-MB-231 cells were decreased by si-GALNT6 transfection but increased by miR-1205 inhibitor transfection ($p < 0.001$, Figure 6 A). Moreover, combined transfection with si-GALNT6 + the miR-1205 inhibitor partially enhanced *GALNT6* expression compared to the transfection with si-GALNT6 alone. CCK-8 and transwell assays revealed that the proliferative and invasive capac-

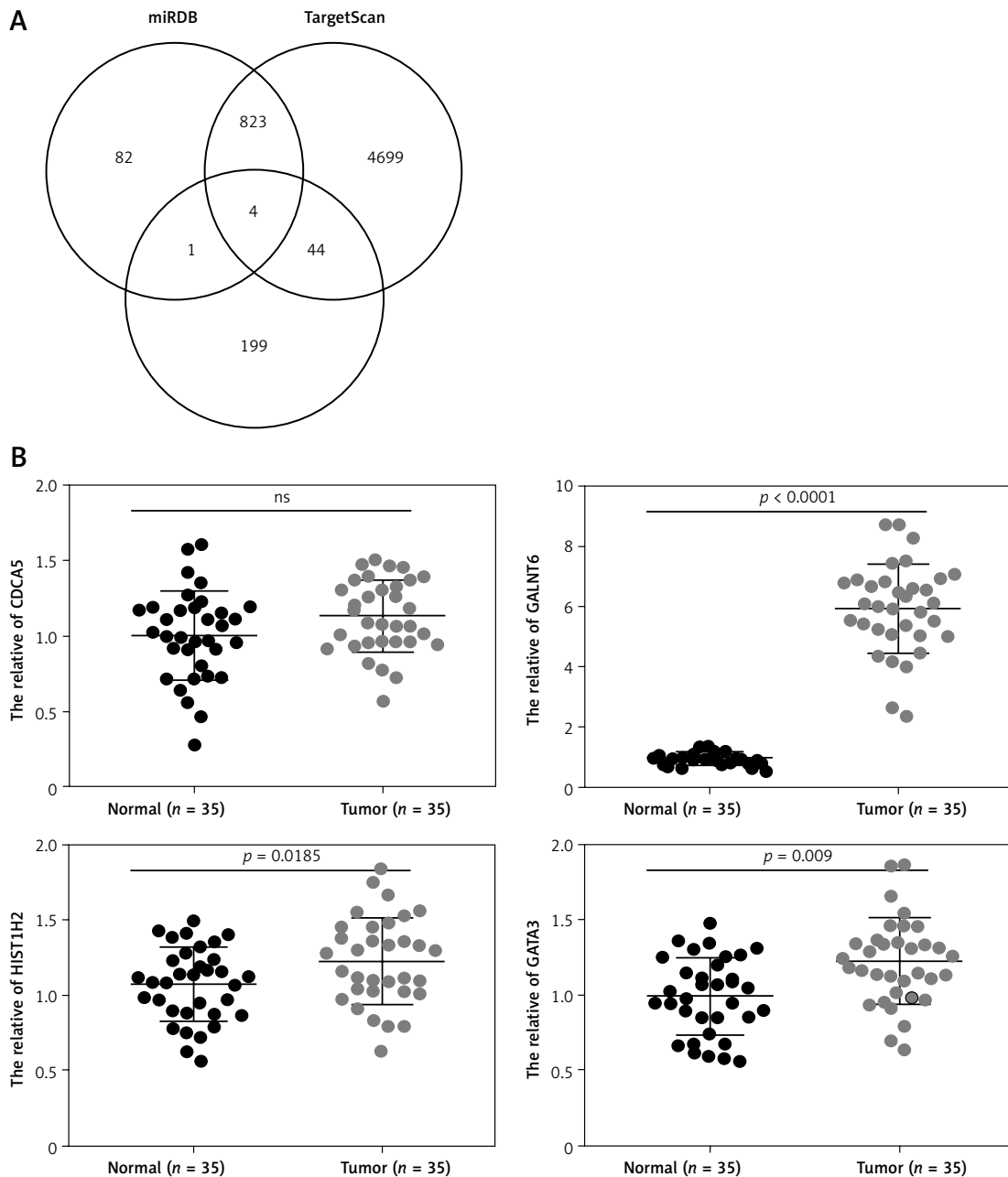
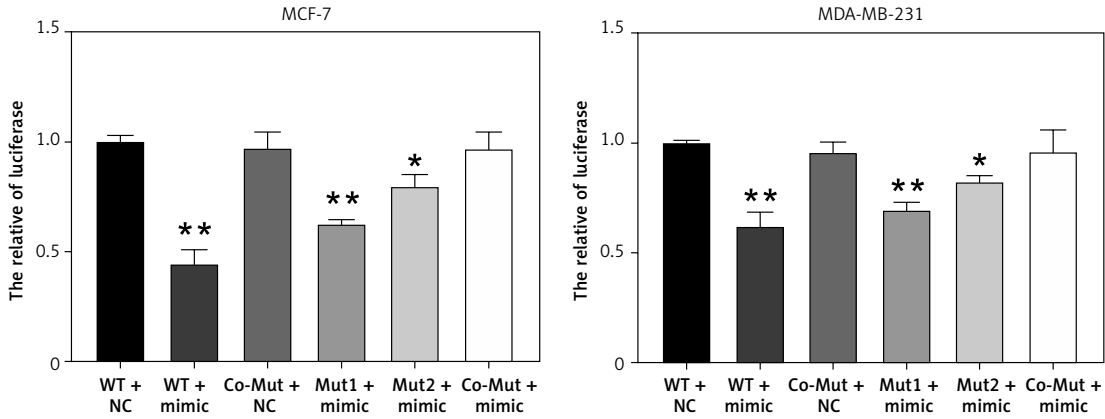


Figure 5. *GALNT6* was a *miR-1205* target. **A** – Four genes (*CDC45*, *GALNT6*, *HIST1H2BK*, and *GATA3*) were overlapping in miRDB, TargetScan and GEPIA. **B** – The expression levels of these four genes in tumoral and normal tissues were determined through RT-qPCR

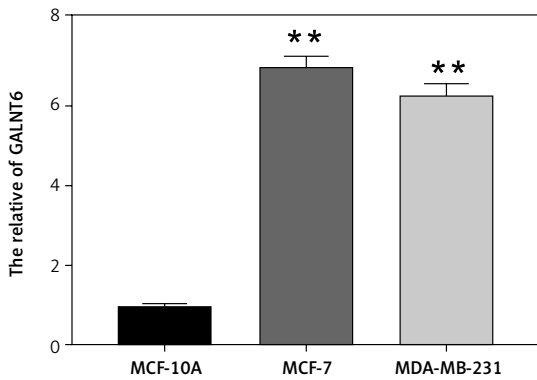
C



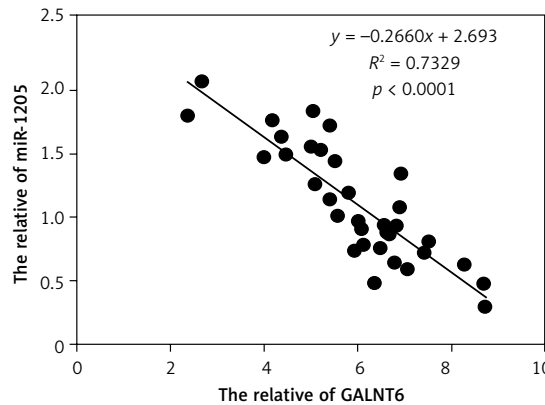
D



E



F



G

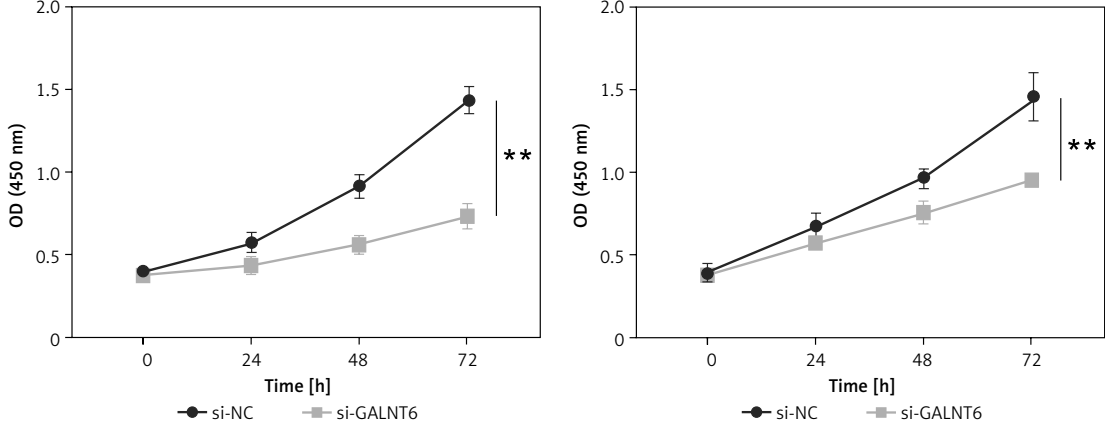


Figure 5. Cont. **C** – The binding sites between GALNT6 and miR-1205 were identified using TargetScan. **D** – The interaction of GALNT6 with miR-1205 was validated via the dual-luciferase reporter experiment, * $p < 0.05$, ** $p < 0.001$ when compared to WT + NC. **E** – The GALNT6 expression levels in MDA-MB-231, MCF-7, and MCF-10A cells were quantified via RT-qPCR, ** $p < 0.001$ vs. MCF-10A. **F** – MiR-1205's expression in tumors had an inverse correlation with that of GALNT6. **G** – GALNT6 silencing's effect on the proliferative abilities of the cells was assessed by means of the CCK-8 experiment, ** $p < 0.001$ vs. si-NC

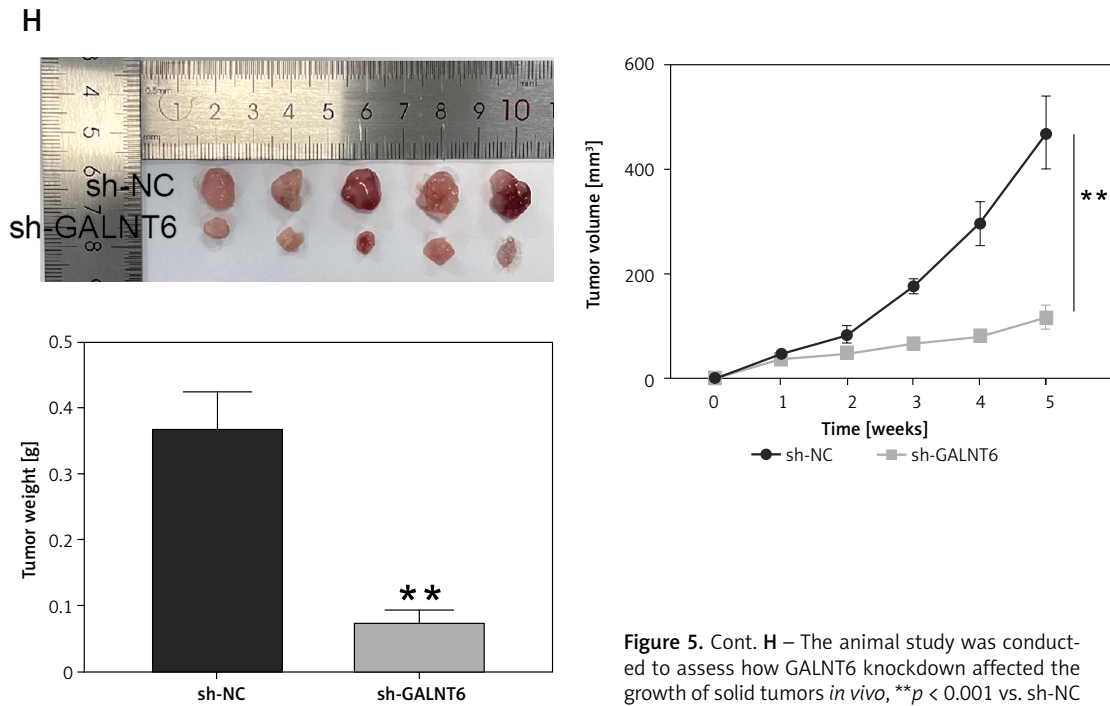


Figure 5. Cont. H – The animal study was conducted to assess how GALNT6 knockdown affected the growth of solid tumors *in vivo*, $**p < 0.001$ vs. sh-NC

ities of cells were considerably decreased in cells transfected with si-GALNT6 alone and increased in cells transfected with the *miR-1205* inhibitor ($p < 0.001$, Figures 6 B and C). Furthermore, repression of cell invasion and proliferation by *GALNT6* knockdown was substantially reversed by the inhibition of *miR-1205*. Cells transfected with si-GALNT6 exhibited enhanced apoptosis, whereas those transfected with the *miR-1205* inhibitor exhibited decreased apoptosis ($p < 0.001$; Figure 6 D). Notably, the effects of *GALNT6* knockdown were reversed by *miR-1205* inhibition. These results indicate that *miR-1205* inhibition aggravates the malignant behaviors of breast cancer cells via the enrichment of *GALNT6*.

Discussion

The main finding of this study was the aberrant overexpression of *circ_0119412* in breast cancer cell lines and tumor specimens. We observed that the downregulation of *circ_0119412* expression inhibited the malignant phenotypes of cancer cells and decreased the tumor growth *in vivo*. *circ_0119412* was found to regulate breast cancer development by targeting the *miR-1205/GALNT6* pathway. This study illustrates the functions of *circ_0119412* in breast cancer and suggests its underlying action mechanisms.

Several circRNAs, such as *circ_0061825*, *circ_0025202*, and *circ_0007294*, have been demonstrated to play important roles and affect the growth, invasion, migration, and chemoresistance of breast cancer cells [24–26]. These findings

reveal the vital roles of circRNAs in breast cancer tumorigenesis. A previous study reported the increased expression of *Circ_0119412* in gastric cancer, and further clinical data suggested its diagnostic value for gastric cancer [15]. *Circ_0119412* overexpression has also been reported in colorectal and ovarian cancers, where its downregulation markedly hampered the migration, proliferation, and invasion of cancer cells [27, 28]. To the best of our knowledge, this is the first study to investigate the specific roles of *circ_0119412* in breast cancer. Consistent with previous reports, we observed increased expression levels of *circ_0119412* in breast cancer tumor specimens in this study. Functional assays revealed that *circ_0119412* knockdown repressed the proliferation and invasion, stimulated the apoptosis, and impeded the tumor growth *in vivo*. Many studies have reported the carcinogenic roles of *circ_0119412* in various cancers, suggesting its targeted inhibition as a potential strategy for cancer treatment.

Here, we identified *miR-1205* as a downstream target of *circ_0119412*. *miR-1205* expression was negatively correlated with *circ_0119412* expression in tumor specimens. Moreover, *miR-1205* expression levels were markedly increased in *circ_0119412* knockdown breast cancer cells, suggesting that *circ_0119412* acts as a sponge and sequesters *miR-1205*. *miR-1205* is also a target of circRNA Ras association domain family member 2 (*RASSF2*) [29]. *miR-1205* enrichment has been reported to alleviate the malignant behaviors of breast cancer cells that are aggravated by circRNA-*RASSF2* overexpression [29]. Consistently,

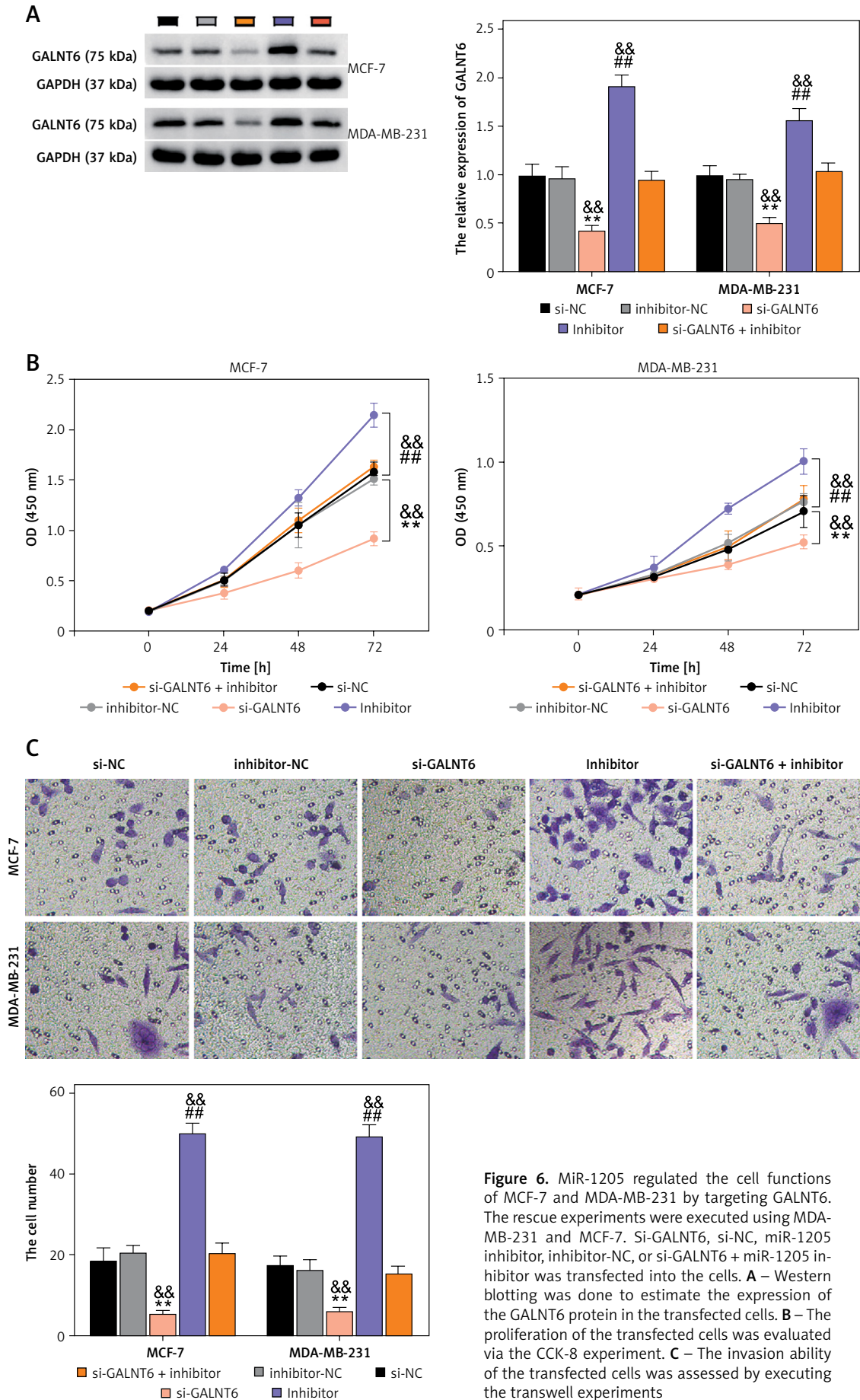


Figure 6. MiR-1205 regulated the cell functions of MCF-7 and MDA-MB-231 by targeting GALNT6. The rescue experiments were executed using MDA-MB-231 and MCF-7. Si-GALNT6, si-NC, miR-1205 inhibitor, inhibitor-NC, or si-GALNT6 + miR-1205 inhibitor was transfected into the cells. **A** – Western blotting was done to estimate the expression of the GALNT6 protein in the transfected cells. **B** – The proliferation of the transfected cells was evaluated via the CCK-8 experiment. **C** – The invasion ability of the transfected cells was assessed by executing the transwell experiments

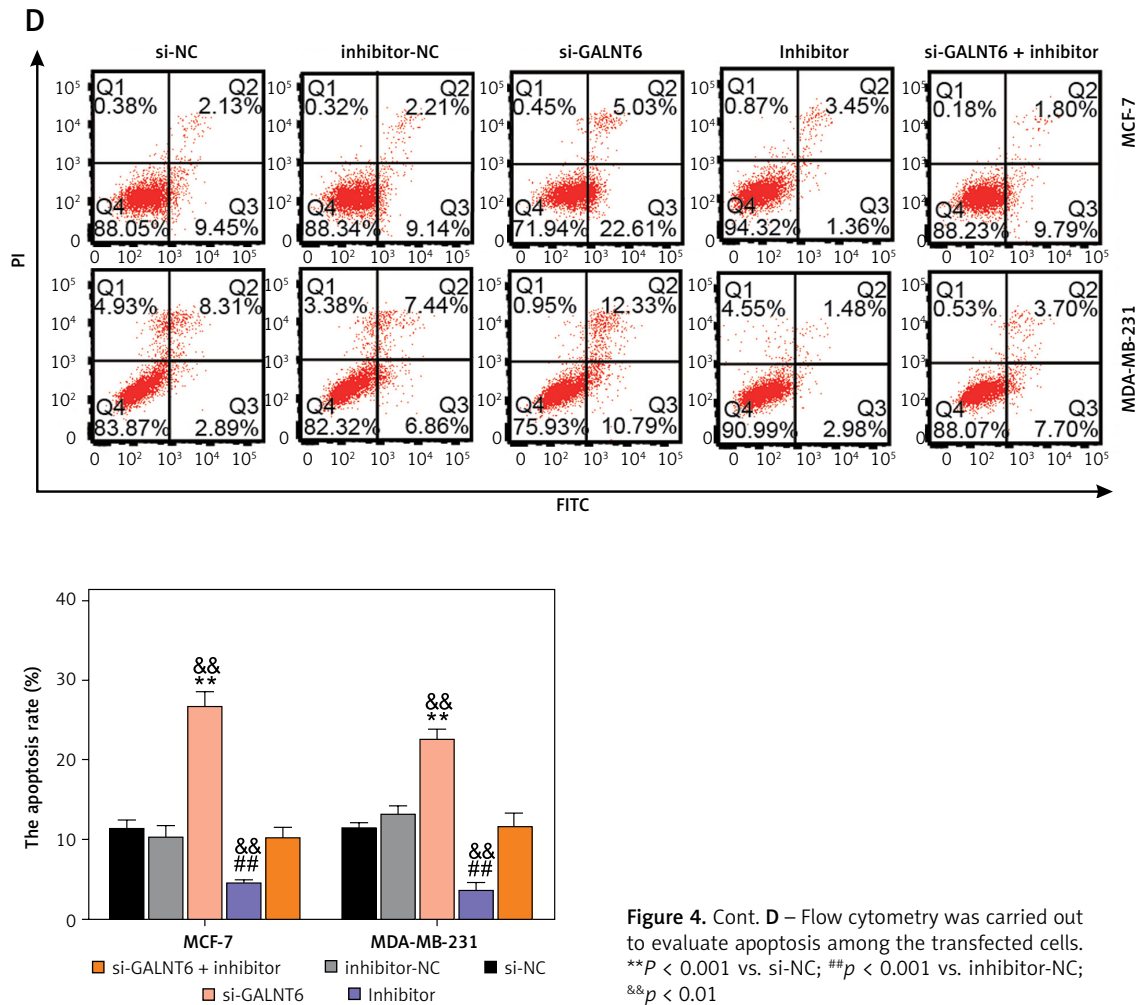


Figure 4. Cont. D – Flow cytometry was carried out to evaluate apoptosis among the transfected cells. ** $P < 0.001$ vs. si-NC; ## $p < 0.001$ vs. inhibitor-NC; && $p < 0.01$

we observed decreased expression levels of *miR-1205* in breast cancer cell lines and tumors in this study. Moreover, inhibition of *miR-1205* aggravated the malignant behaviors of breast cancer cells and partially reversed the effects of *circ_0119412* knockdown. Therefore, *circ_0119412* may promote breast cancer progression by depleting *miR-1205*.

GALNT6 plays important roles in carcinogenesis. *GALNT6* expression is remarkably high and associated with advanced TNM stage and distant metastasis in patients with gastric cancer [30]. High *GALNT6* expression predicts poor prognosis in patients with ovarian cancer [31]. Increased *GALNT6* expression has also been reported in breast cancer [32, 33]. Increased expression of *GALNT6* is associated with poor prognosis, and its knockdown inhibits the growth of breast cancer cells [32, 33]. Additionally, *GALNT6* has been reported to induce breast cancer tumorigenesis and metastasis *in vivo* [21, 22]. In this study, *GALNT6* was found to be a target of *miR-1205*. Knockdown of *GALNT6* repressed proliferation and invasion and enhanced the apoptosis of breast cancer cells. Rescue experiments further revealed that *miR-1205* binds to *GALNT6* and inhibits its function.

Being a preliminary study exploring the roles of *circ_0119412* in breast cancer, this work has some limitations. Whether *circ_0119412* overexpression exerts effects antagonistic to those of *circ_0119412* downregulation remains unclear and requires further investigation. Moreover, the findings of our study require further validation. Future studies should explore other miRNAs potentially targeted by *circ_0119412* to enrich its regulatory networks.

In conclusion, in this study, we demonstrated the abnormally increased expression of *circ_0119412* in breast cancer via regulation of the *miR-1205/GALNT6* pathway. To the best of our knowledge, this study is the first to reveal the specific roles of *circ_0119412* in breast cancer. Our findings provide novel insights into the pathogenesis of breast cancer and suggest targeted inhibition of *circ_0119412* as a promising strategy for breast cancer treatment.

Acknowledgments

Jianhua Liu and Qiuli Du equally contributed to this work.

Funding

No external funding.

Ethical approval

Approval number: W202111-35.

Conflict of interest

The authors declare no conflict of interest.

References

1. Sung H, Ferlay J, Siegel RL, et al. Global cancer statistics 2020: GLOBOCAN estimates of incidence and mortality worldwide for 36 cancers in 185 countries. *CA Cancer J Clin* 2021; 71: 209-49.
2. Rivera E, Gomez H. Chemotherapy resistance in metastatic breast cancer: the evolving role of ixabepilone. *Breast Cancer Res* 2010; 12 (Suppl 2): S2.
3. Al-Mahmood S, Sapiezynski J, Garbuzenko OB, Minko T. Metastatic and triple-negative breast cancer: challenges and treatment options. *Drug Deliv Transl Res* 2018; 8: 1483-507.
4. Weigelt B, Reis-Filho JS. Histological and molecular types of breast cancer: is there a unifying taxonomy? *Nat Rev Clin Oncol* 2009; 6: 718-30.
5. Goh JN, Loo SY, Datta A, et al. microRNAs in breast cancer: regulatory roles governing the hallmarks of cancer. *Biol Rev Camb Philos Soc* 2016; 91: 409-28.
6. Banin Hirata BK, Oda JM, Losi Guembarovski R, Ariza CB, de Oliveira CE, Watanabe MA. Molecular markers for breast cancer: prediction on tumor behavior. *Dis Markers* 2014; 2014: 513158.
7. Greene J, Baird AM, Brady L, et al. Circular RNAs: biogenesis, function and role in human diseases. *Front Mol Biosci* 2017; 4: 38.
8. Liu J, Liu T, Wang X, He A. Circles reshaping the RNA world: from waste to treasure. *Mol Cancer* 2017; 16: 58.
9. Bolha L, Ravnik-Glavač M, Glavač D. Circular RNAs: biogenesis, function, and a role as possible cancer biomarkers. *Int J Genomics* 2017; 2017: 6218353.
10. Yin WB, Yan MG, Fang X, Guo JJ, Xiong W, Zhang RP. Circulating circular RNA hsa_circ_0001785 acts as a diagnostic biomarker for breast cancer detection. *Clin Chim Acta* 2018; 487: 363-8.
11. Xu Y, Yao Y, Leng K, et al. Increased expression of circular RNA circ_0005230 indicates dismal prognosis in breast cancer and regulates cell proliferation and invasion via miR-618/CBX8 signal pathway. *Cell Physiol Biochem* 2018; 51: 1710-22.
12. He D, Yang X, Kuang W, Huang G, Liu X, Zhang Y. The novel circular RNA Circ-PGAP3 promotes the proliferation and invasion of triple negative breast cancer by regulating the miR-330-3p/Myc Axis. *Onco Targets Ther* 2020; 13: 10149-59.
13. Dou D, Ren X, Han M, et al. CircUBE2D2 (hsa_circ_0005728) promotes cell proliferation, metastasis and chemoresistance in triple-negative breast cancer by regulating miR-512-3p/CDCA3 axis. *Cancer Cell Int* 2020; 20: 454.
14. Cao L, Wang M, Dong Y, et al. Circular RNA circRNF20 promotes breast cancer tumorigenesis and Warburg effect through miR-487a/HIF-1 α /HK2. *Cell Death Dis* 2020; 11: 145.
15. Wei J, Wei W, Xu H, et al. Circular RNA hsa_circRNA_102958 may serve as a diagnostic marker for gastric cancer. *Cancer Biomark* 2020; 27: 139-45.
16. Panda AC. Circular RNAs act as miRNA Sponges. *Adv Exp Med Biol* 2018; 1087: 67-79.
17. Dudekula DB, Panda AC, Grammatikakis I, De S, Abdelmohsen K, Gorospe M. CircInteractome: a web tool for exploring circular RNAs and their interacting proteins and microRNAs. *RNA Biol* 2016; 13: 34-42.
18. Yan H, Chen X, Li Y, et al. MiR-1205 functions as a tumor suppressor by disconnecting the synergy between KRAS and MDM4/E2F1 in non-small cell lung cancer. *Am J Cancer Res* 2019; 9: 312-29.
19. Yang M, Li G, Fan L, Zhang G, Xu J, Zhang J. Circular RNA circ_0034642 elevates BATF3 expression and promotes cell proliferation and invasion through miR-1205 in glioma. *Biochem Biophys Res Commun* 2019; 508: 980-5.
20. Lee S, Vasudevan S. Post-transcriptional stimulation of gene expression by microRNAs. *Adv Exp Med Biol* 2013; 768: 97-126.
21. Liu C, Li Z, Xu L, et al. GALNT6 promotes breast cancer metastasis by increasing mucin-type O-glycosylation of α 2M. *Aging (Albany NY)* 2020; 12: 11794-811.
22. Mao Y, Zhang Y, Fan S, et al. GALNT6 promotes tumorigenicity and metastasis of breast cancer cell via β -catenin/MUC1-C signaling pathway. *Int J Biol Sci* 2019; 15: 169-82.
23. Lin TC, Chen ST, Huang MC, et al. GALNT6 expression enhances aggressive phenotypes of ovarian cancer cells by regulating EGFR activity. *Oncotarget* 2017; 8: 42588-601.
24. Pan G, Mao A, Liu J, Lu J, Ding J, Liu W. Circular RNA hsa_circ_0061825 (circ-TFF1) contributes to breast cancer progression through targeting miR-326/TFF1 signalling. *Cell Prolif* 2020; 53: e12720.
25. Sang Y, Chen B, Song X, et al. circRNA_0025202 regulates tamoxifen sensitivity and tumor progression via regulating the miR-182-5p/FOXO3a axis in breast cancer. *Mol Ther* 2019; 27: 1638-52.
26. Zeng K, He B, Yang BB, et al. The pro-metastasis effect of circANKS1B in breast cancer. *Mol Cancer* 2018; 17: 160.
27. Li R, Wu B, Xia J, Ye L, Yang X. Circular RNA hsa_circRNA_102958 promotes tumorigenesis of colorectal cancer via miR-585/CDC25B axis. *Cancer Manag Res* 2019; 11: 6887-93.
28. Wang G, Zhang H, Li P. Upregulation of hsa_circRNA_102958 indicates poor prognosis and promotes ovarian cancer progression through miR-1205/SH2D3A axis. *Cancer Manag Res* 2020; 12: 4045-53.
29. Zhong W, Bao L, Yuan Y, Meng Y. CircRASSF2 acts as a prognostic factor and promotes breast cancer progression by modulating miR-1205/HOXA1 axis. *Bioengineered* 2021; 12: 3014-28.
30. Guo Y, Shi J, Zhang J, Li H, Liu B, Guo H. Polypeptide N-acetylgalactosaminyltransferase-6 expression in gastric cancer. *Onco Targets Ther* 2017; 10: 3337-44.
31. Sheta R, Bachvarova M, Plante M, et al. Altered expression of different GalNAc-transferases is associated with disease progression and poor prognosis in women with high-grade serous ovarian cancer. *Int J Oncol* 2017; 51: 1887-97.
32. Park JH, Nishidate T, Kijima K, et al. Critical roles of mucin 1 glycosylation by transactivated polypeptide N-acetylgalactosaminyltransferase 6 in mammary carcinogenesis. *Cancer Res* 2010; 70: 2759-69.
33. Kimura R, Yoshimaru T, Matsushita Y, et al. The GALNT6-LGALS3BP axis promotes breast cancer cell growth. *Int J Oncol* 2020; 56: 581-95.